PERFORMANCE ANALYSIS OF A FOUR-STROKE COMPRESSED AIR ENGINE

Fancong Zeng[1, *], Jinli Xu[1*]

[*1]School of Mechanical and Electrical Engineering, Wuhan University of Technology, Wuhan, China

[*] Corresponding author; E-mail: xujingli2018@163.com

The purpose of this paper is to investigate working performance for a four-stroke compressed air engine (CAE) via numerical studies. A mathematical model is developed to study the influence of several operative parameters on working performance. The mathematical model consists of thermodynamic model, each stroke model and dynamic model. In addition, a working principle and an experimental system of the CAE are set up. The aims are to (1) introduce the novel four-stroke engine, and (2) quantify the influence of rotational speed, supply pressure and supply temperature on working characteristics. The simulation and analysis show several meaningful results. The CAE has higher cylinder pressure and work efficiency in lower speed stage, and the increase of the supply pressure can effectively improve indicated work and work efficiency. However, supply temperature has little effect on the performance of the CAE. Therefore, the study of this work will provide a certain guidance function for further study on optimizing design of the CAE.

Key words*: Compressed air engine, Four-stroke, Working performance, Mathematical model*

1. Introduction

Over the recent decades, reducing carbon dioxide (CO_2) emission is a crucial issue worldwide. Exhaust gas from internal combustion (IC) engines contributes largely to CO_2 emissions, and it has become increasingly important to find environmentally friendly energies to replace conventional fossil fuels [1]. Compressed air, as an energy medium, has some distinct benefits for its zero CO_2 emission and convenience in storage, transportation and conversion [2-3]. Compressed air has found vast applications in fields such as electricity generation, vehicle engines and energy storage technologies [4-6]. Among them the compressed air engine (CAE) has a direct and common connection with human society and life and so, it attracts substantial attention [7,8].

Compared with other kind of fuels, compressed air has the following advantages. Its resources are vast and it can be generated through several ways such as solar energy, wind energy and tidal energy. A CAE has both the advantages of the non-burning fuel and the zero pollution. The cost of a CAE is much less than a fuel cell and an IC engine, though they have higher efficiencies than CAEs. IC engines can be simply modified to CAEs if its structure gets a slight change. The type of the CAE in this study is a four-stroke piston-type CAE, and the working process is basically the same as the conventional IC engine. Compressed air expands in the engine cylinder, it can convert the reciprocal motion of piston into one-way rotary motion of the output shaft, and discharges in the form of pure air at low temperature.

AirPod, a green energy car, was invented by a French company of air-powered vehicles, in the 1990s, it was the successful application of a CAE [9]. The existing literatures showed that a great deal of investigations on kinds of CAEs had been conducted by Chinese research scholars in the past 10 years [10-14]. Liu et al. [10] reported that compressed air have similar energy density as Ni-H battery, the circulation efficiency of compressed air was 25%–32.3% in practice and the characteristics of the CAE was suitable for driving a vehicle. Yu et al. [11] performed the analysis of the energy efficiency and the output power of the CAE, and an improved NSGA-II was introduced to optimize the energy efficiency of the engine with the given output power. Yu et al. [12] also studied two kinds of compressed air engines: single cylinder piston-type CAE (SCAE) and double crank link CAE (DCAE), the average output power and efficiency characteristics of two kinds of CAEs were obtained by simulation and experiment, and the DCAE could improve the CAE performance under high rotational speeds. In Yu's another literature [13], the mathematical model was setup through analysis of the working process of a two-stroke CAE, and experiments were carried out to verify the engine performance. The mathematical model was transformed to a dimensionless expression. The dimensionless speed and efficiency characteristics of the CAE were obtained in his paper. Liu et al. [14] proposed a CAE consisting of one small and one large cylinder to conduct two-stage expansion in series, by fully using the high-pressure air and increasing the power output and efficiency of the CAE. But few studies established complete working process models of the four-stroke CAE, as well as methods to analyze the performance under critical working parameters.

Several studies provided references for the performance analysis of the four-stroke CAE. The working process mathematical model of the two working modes of hybrid four-stroke compressed-air and fuel engine were respectively established [15]. The adjustable expansion ratio was considered in the research of the CAE [16]. However, no experiments or in-depth discussion was reported for this special study. Therefore, the theoretical model of the four-stroke CAE is established in this paper for performance analysis and the design of the CAE.

2. Mathematical model of the CAE

As shown in Figure. 1, intake valves and exhaust valves are controlled by the valve system. At the beginning of the intake stroke, the intake valves open immediately, and the atmosphere flows into the cylinder through the intake valves because of the pressure difference. When the piston is near the bottom dead center (BDC), the intake valves close. In the compression stroke, the piston moves up near the top dead center (TDC). In the inflation and expansion stroke, the high-frequency electromagnetic valve and the air nozzle begin to work, then the compressed air flows into the cylinder through the air nozzle, and pushes the piston downwards. After a specific crank angle, the high-frequency electromagnetic valve and the air nozzle close while the compressed air expands to push the piston down and output work. When the piston moves back to the bottom dead center (BDC), the exhaust valves open so that residual air discharges under the impetus of the piston. After the piston moves back to the top dead center (TDC), the four-stroke CAE completes a complete work cycle.

The CAE cylinder can be seen to be a thermodynamic system, and the following assumptions are made [17]. First, the compressed air is ideal, which means specific heat and specific enthalpy are only related to the temperature. Second, the changes of kinetic and gravitational energy are negligible. Third, the process of gas flowing into/out of the cylinder is a quasi-steady one. Finally, there is no leak or friction during the working process.

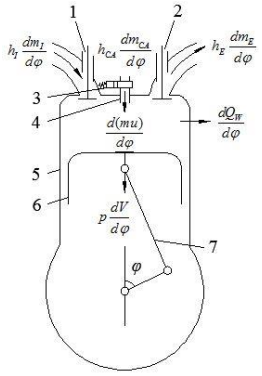

1. Intake valve 2. Exhaust valve 3. High-frequency electromagnetic valve 4. Air nozzle
5. Cylinder 6. Piston 7. Crank-link mechanism

Fig. 1 Structure and thermodynamic analysis diagram of four-stroke CAE

2.1 Thermodynamic model

The energy equation can be expressed as

$$\frac{dU}{d\varphi}=\frac{dQ_w}{d\varphi}+h_I\frac{dm_I}{d\varphi}+h_{CA}\frac{dm_{CA}}{d\varphi}+h_E\frac{dm_E}{d\varphi}+\frac{dW}{d\varphi} \tag{1}$$

Where U is the internal energy of the air in the cylinder; Q_w is the heat absorbed by the air from the cylinder walls; h_j *(j=I, E, CA)* are the specific enthalpies of intake air, exhaust air and injection compressed air, respectively; m_j*(j=I, E, CA)* are the mass of intake air, exhaust air and injection compressed air, respectively; W is the mechanical work on the piston; φ is the crank angle.

U can be written in this form

$$dU=d(m\cdot u)=udm+mdu \tag{2}$$

Where m is the mass of the air in the cylinder; u is the specific heat.

For ideal air, u can be seen as a function of air temperature, that is $u=u(T)$, and u can be written in a fully differential form

$$\frac{du}{d\varphi}=\frac{\partial u}{\partial T}\frac{dT}{d\varphi}=c_v\frac{dT}{d\varphi} \tag{3}$$

Where c_v is the constant volume specific heat; T is the temperature of the air in the cylinder.

The heat transfer in the process can be expressed as

$$\frac{dQ_w}{d\varphi}=\frac{1}{\omega}\sum_{i=1}^{3}a_g\cdot A_i(T_{wi}-T) \tag{4}$$

Where ω is the angular speed of the crank shaft; a_g is the heat transfer coefficie; A_i is the total heat transfer area; T_{wi} *(i=1, 2, 3)*are the temperatures of the cylinder head, the piston and the cylinder liner, respectively.

The coefficient of the heat transfer between the air and the cylinder walls is given as

$$a_g=0.1129\cdot D^{-0.2}\cdot p^{0.8}\cdot(Sn/30)^{0.8}\cdot T^{-0.594} \tag{5}$$

Where D is the diameter of the cylinder; p is the pressure of the air in the cylinder; S is the stroke of the piston; n is the rotational speed of the CAE.

The mechanical work by the compressed air is described by

$$\frac{dW}{d\varphi}=-p\frac{dV}{d\varphi} \tag{6}$$

Where V is the cylinder volume.

The cylinder volume V can be written as

$$V = \frac{\pi D^2}{4}\{\frac{S}{\varepsilon - 1} + \frac{S}{2}[(1 + \frac{1}{\lambda}) - \cos\varphi - \frac{1}{\lambda}\sqrt{1 - \lambda^2 \cdot \sin^2\varphi}]\} \tag{7}$$

Where ε is the compression ratio; λ is the ratio of crank radius to connecting rod.

The change rate of the cylinder volume can be expressed as

$$\frac{dV}{d\varphi} = \frac{\pi \cdot D^2 \cdot S}{8}[\sin\varphi + \frac{\lambda}{2}\frac{\sin(2 \cdot \varphi)}{\sqrt{1 - \lambda^2 \sin^2\varphi}}] \tag{8}$$

Substituting equations (2)–(6) into equation (1) yields the following differential equation

$$\frac{dT}{d\varphi} = \frac{1}{m \cdot c_v}(\frac{dQ_w}{d\varphi} - p\frac{dV}{d\varphi} + h_I \cdot \frac{dm_I}{d\varphi} + h_{CA} \cdot \frac{dm_{CA}}{d\varphi} + h_E \cdot \frac{dm_E}{d\varphi} - u\frac{dm}{d\varphi}) \tag{9}$$

The mass air flow of the CAE can be expressed as

$$\frac{dm_j}{d\varphi} = \frac{1}{\omega} \cdot \mu F\sqrt{\frac{p_1}{v_1}} \cdot \psi \tag{10}$$

Where μ is the coefficient of discharge; F is the effective sectional area; p_1 is the upstream pressure; v_1 is the upstream air specific volume; ψ is the flow function.

When $\frac{p_r}{p_1} > (\frac{2}{k+1})^{\frac{k}{k-1}}$, the air flow state is sub-sonic flow state, and the flow function ψ can be written as

$$\psi = \sqrt{\frac{2k}{k-1}[(\frac{p_r}{p_1})^{\frac{2}{k}} - (\frac{p_r}{p_1})^{\frac{k+1}{k}}]} \tag{11}$$

Where k is the adiabatic exponent of the air; p_r is the downstream pressure.

When $\frac{p_r}{p_1} \le (\frac{2}{k+1})^{\frac{k}{k-1}}$, the air flow state is sonic flow state, and the flow function ψ can be written as

$$\psi = (\frac{2}{k+1})^{\frac{1}{k-1}}\sqrt{\frac{2k}{k+1}} \tag{12}$$

The ideal gas equation of state can be derived as

$$pV = mRT \tag{13}$$

Here, R is the gas constant of air.

2.2 Compression stroke

During the compression stroke, the intake valves and exhaust valves are closed, because it is assumed that gas has no leak, the mass air flow of the CAE can be considered to be zero.

$$\frac{dm_I}{d\varphi} = 0,\ \frac{dm_{CA}}{d\varphi} = 0\ ,\ \frac{dm_E}{d\varphi} = 0 \tag{14}$$

The energy conservation equation can be expressed as

$$\frac{dT}{d\varphi} = \frac{1}{mc_v}(\frac{dQ_w}{d\varphi} - p\frac{dV}{d\varphi}) \tag{15}$$

Simultaneously, the ideal gas equation of state can be rewritten as

$$\frac{dp}{d\varphi} = p(\frac{1}{T}\frac{dT}{d\varphi} - \frac{1}{V}\frac{dV}{d\varphi}) \tag{16}$$

2.3 Inflation and expansion stroke

Inflation and expansion stroke can be divided into two stages, namely the inflating stage and the expansion stage. During the inflating stage, the intake valves and exhaust valves are closed, and compressed air is charged into the cylinder. In this stage, the change of the gas mass in the cylinder is the mass change of the compressed air injecting into the cylinder.

The mass conservation equation can be expressed as

$$\frac{dm}{d\varphi}=\frac{dm_{CA}}{d\varphi} \tag{17}$$

The energy conservation equation can be expressed as

$$\frac{dT}{d\varphi}=\frac{1}{mc_v}(\frac{dQ_w}{d\varphi}-p\frac{dV}{d\varphi}+h_{CA}\frac{dm_{CA}}{d\varphi}-u\frac{dm}{d\varphi}) \tag{18}$$

The ideal gas equation of state can be rewritten as

$$\frac{dp}{d\varphi}=\frac{1}{V}\left[R\left(\frac{dm}{d\varphi}T+\frac{dT}{d\varphi}m\right)-p\frac{dV}{d\varphi}\right] \tag{19}$$

During the expansion stage, the intake valves, the exhaust valves and the air nozzle are all closed. Similar to the compression stage, the gas mass in the cylinder remains unchanged.

The mass conservation equation can be expressed as

$$\frac{dm}{d\varphi}=0 \tag{20}$$

The energy conservation equation can be expressed as

$$\frac{dT}{d\varphi}=\frac{1}{mc_v}(\frac{dQ_w}{d\varphi}-p\frac{dV}{d\varphi}) \tag{21}$$

The ideal gas equation of state can be rewritten as

$$\frac{dp}{d\varphi}=p(\frac{1}{T}\frac{dT}{d\varphi}-\frac{1}{V}\frac{dV}{d\varphi}) \tag{22}$$

2.4 Exhaust stroke

During the exhaust stroke, the intake valves are closed while the exhaust valves are open, and the change of the gas mass in the cylinder is the mass change of the residual air flowing out of the cylinder.

The mass conservation equation can be expressed as

$$\frac{dm}{d\varphi}=\frac{dm_E}{d\varphi} \tag{23}$$

The energy conservation equation can be expressed as

$$\frac{dT}{d\varphi}=\frac{1}{mc_v}(\frac{dQ_w}{d\varphi}-p\frac{dV}{d\varphi}-h_E\frac{dm_E}{d\varphi}-u\frac{dm}{d\varphi}) \tag{24}$$

The ideal gas equation of state can be rewritten as

$$\frac{dp}{d\varphi}=\frac{1}{V}\left[R\left(\frac{dm}{d\varphi}T+\frac{dT}{d\varphi}m\right)-p\frac{dV}{d\varphi}\right] \tag{25}$$

2.5 Intake stroke

During the intake stroke, the intake valves are open while the exhaust valves are closed, and the change of the gas mass in the cylinder is the mass change of the common air flowing into the cylinder.

The mass conservation equation can be expressed as

$$\frac{dm}{d\varphi}=\frac{dm_I}{d\varphi} \tag{26}$$

The energy conservation equation can be expressed as

$$\frac{dT}{d\varphi}=\frac{1}{mc_v}\left(\frac{dQ_w}{d\varphi}-p\frac{dV}{d\varphi}+h_I\frac{dm_I}{d\varphi}-u\frac{dm}{d\varphi}\right) \tag{27}$$

The ideal gas equation of state can be rewritten as

$$\frac{dp}{d\varphi}=\frac{1}{V}\left[R\left(\frac{dm}{d\varphi}T+\frac{dT}{d\varphi}m\right)-p\frac{dV}{d\varphi}\right] \tag{28}$$

In the numerical calculation, the processes of four strokes are computed using the fourth order Runge-Kutta method, and the theoretical computing results are closer to the actual operation of the CAE [18].

2.6 Dynamic model

From the force analysis of the crank-link mechanism, and the output torque of the CAE can be expressed as

$$M=\frac{(p-p_0)A_h-m_d r\omega^2(\cos\varphi+\lambda\cos 2\varphi)}{\cos\beta} \tag{29}$$

Where p_0 is the atmospheric pressure; A_h is the projected area of the piston; m_d is the mass the crank-link mechanism; r is the radius of the crank; β is the angle between the connecting rod and the axis of the cylinder, $\sin\beta=\lambda\sin\varphi$.

2.7 Key performance parameters

The calculations and analyses of relevant performance can be calculated by the following equations.

(1) The indicated work of single cylinder per cycle W_i

$$W_i=\int_{cyc}p\cdot\frac{dV}{d\varphi}\cdot d\varphi \tag{30}$$

(2) The average effective torque of single cylinder M_e

$$M_e=\eta_m\cdot\frac{1}{4\pi}\int_{cyc}M d\varphi \tag{31}$$

Where η_m is the mechanical efficiency.

(3) The effective power of the CAE P_e

$$P_e=\frac{\frac{\pi}{4}D^2\cdot S\times 10^3\cdot n\cdot i\cdot p_{me}}{30\cdot\tau} \tag{32}$$

Where p_{me} is the average effective pressure; i is the number of cylinders; τ is the number of strokes.

(4) The work efficiency η

$$\eta = \frac{W_i}{W} \cdot \eta_m \tag{33}$$

3. Experimental setup

The development of the four-stroke CAE required orginal system experiments and calibrations on the test bench, in order to accomplish some steady tests of the injection pressure and the injection temperature characteristics. These processes can also verify and test the stability and performance of the CAE. Generally, a CAE test bench is composed of an air compressor, compressed air storage tanks, a pressure reducing valve, supply pressure sensors, cylinder pressure sensors, flow sensors, high-frequency electromagnetic valves, air nozzles, thermocouples, a high-speed data acquisition unit and an engine electronic control unit (ECU). After completing the experiments and verification, the overall test can be conducted, which mainly focuses on output parameters, such as engine power, torque etc. Meanwhile, some other parameters like rotational speed, supply pressure, supply temperature, flow rate, exhaust pressure and exhaust temperature etc. ought to be monitored to adjust the control parameters in real time and protect the CAE from malfunctions. The engine test bench is universally made up of a complete motor, dynamometer and monitoring system. The experimental prototype test bench and measurement equipment are illustrated in Figure. 2.

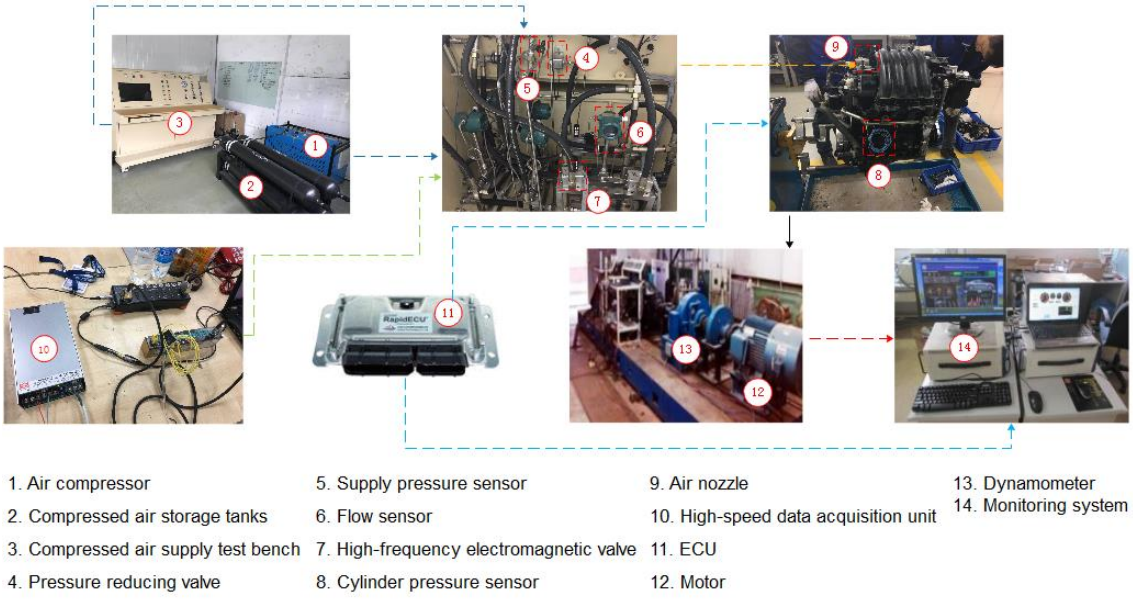

Fig. 2 Experimental prototype test bench and measurement equipment

4. Result and discussion

Working characteristics of the four-stroke CAE can be investigated by cylinder pressure, output torque, average effective torque, effective power, indicated work, work efficiency and so on. Parameters for rotational speed, supply pressure and supply temperature are important to working process simulation. In this paper, the working characteristics and working processes at different initial

conditions are investigated by the mathematical model. The working initial angle of the CAE is compression start angle while simulating working process.

In present work, intake parameters are imposed on the entire computational domain as initial conditions (shown in Table. 1) for numerical simulation. The effect of heat transfer between the outer wall and air is not considered. Thus, wall boundary is in adiabatic condition. Crank angle is at 355°CA, corresponding to the intake angle of the compressed air. Figure. 3 illustrates the port timing diagram of the CAE.

Tab.1 The parameters of the CAE

Parameters	Values
Diameter of the cylinder(mm)	D=69.5
Stroke of the piston(mm)	S=79.5
Ratio of crank radius to connecting rod	λ=0.32
Compression ratio	ε=9.8
Radius of the crank(mm)	r =39
Ambient pressure(bar)	1.01
Ambient temperature(K)	293
Diameter of the intake valve(mm)	25
Diameter of the exhaust valve(mm)	20
Supply pressure(bar)	p_i=20
Rotational speed(r/min)	n=1000
Intake sustain angle(°CA)	50
Exhaust advance angle(°CA)	10

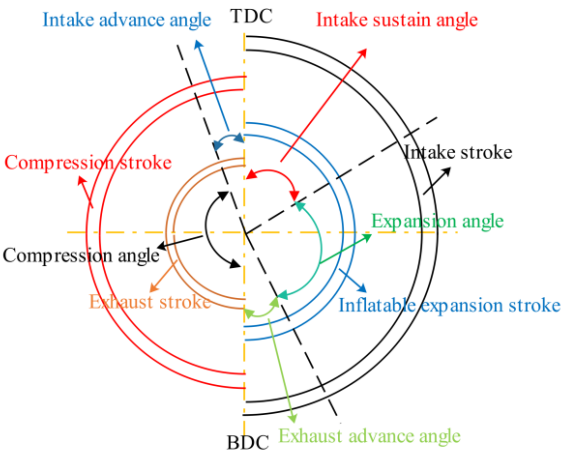

Fig. 3 Port timing diagram of the CAE

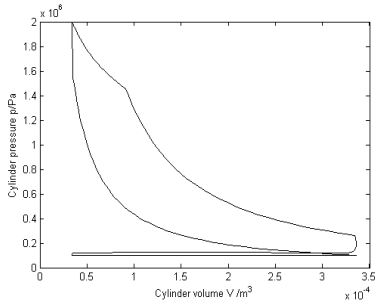

Fig. 4 Indicator diagram

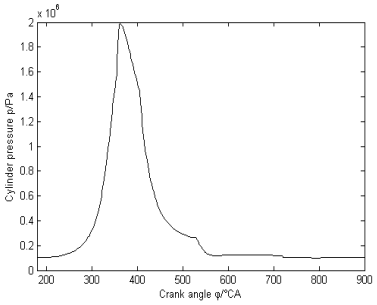

Fig. 5 Cylinder pressure plot

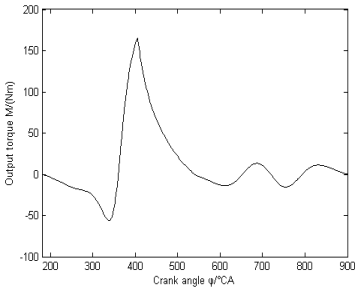

Fig. 6 Output torque plot

As shown in Figure. 4 and Figure. 5, the indicated work and the variation of cylinder pressure in a working cycle are revealed. According to the formula (30), the total pressure volume (*P*-*V*) area represents the value of the indicated work. The cylinder pressure increases rapidly in the compression stage, and the peak cylinder pressure is close to the supply pressure, the pressure drops rapidly in the expansion stage. Figure. 6 shows output torque changing with different crank angles. From this figure, it can be found that the piston moves upward and the piston work is negative in the compression stroke, which results in a negative output torque of the CAE. As the compressed air continuously filled into the cylinder, it continues to push the piston to output the mechanical work on the piston. Thus, the output torque increases. At the end of inflation stage, the output torque reaches the maximum.

4.1 Rotational speed

Figure. 7 illustrates the indicator diagrams at different rotational speeds. From this figure, it can be found that the lower the rotational speed, the larger the indicated work. This is because with the increased rotational speed, the intake time of the compressed air becomes shorter. As a result, air inflow decreases and energy of the compressed air is reduced, which leads to a decrease in the indicator work. Figure. 8 shows the variation of the cylinder pressure under various rotational speeds. It is found that the rotational speed has an obvious effect on cylinder pressure. The higher the rotational speed, the smaller the top pressure of the cylinder. Furthermore, a small variation of rotational speed may result in an evident change of cylinder pressure. While the rotational speed decreases, the appearance of the top pressure has a tendency to move backward, and the pressure at the end of the expansion stage will increase. Consequently, the cylinder pressure will decrease sharply when entering the expansion stage and a steep slope of pressure will follow up. With the increasing of rotational speed, however, this phenomenon will disappear slowly.

The simulation shows that the cylinder temperature varies with the rotational speed changing from 1000r/min to 3000r/min. However, its variation tendency is different from cylinder pressure, that is, the higher the rotational speed, the higher the cylinder temperature at the inflation and expansion stroke and exhaust stroke. Because of the higher the rotational speed, the smaller the mass of the compressed air that flows into the cylinder, this will lead to the lower temperature drop when the air is mixed at the end of the compression stroke. Therefore, the temperature of the mixed air is higher.

The effect of rotational speed to output torque may be analyzed through Figure. 9. It is found that, with the increased rotational speed, the output torque of the CAE is smaller. In the exhaust stroke, the piston pushes the gas and the output torque is negative. However, the exhaust time becomes shorter with the increased rotational speed, so the mass of the residual air is larger. The residual air in the

cylinder becomes the resistance of the exhaust gas, thereby increasing the cylinder pressure, which results in an increase in the reverse output torque of the CAE.

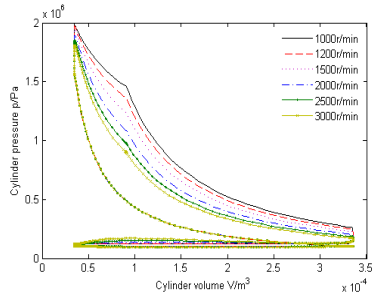

Fig.7 Indicator diagrams at different rotational speeds

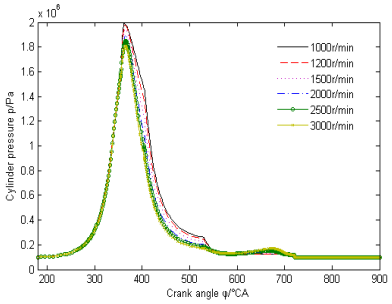

Fig.8 Cylinder pressure variation at different rotational speeds

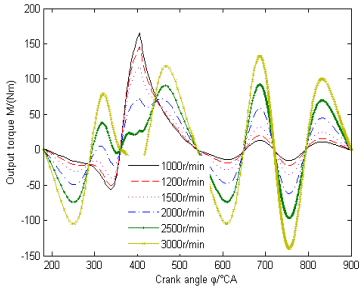

Fig. 9 Output torque variation at different rotational speeds

4.2 Supply pressure

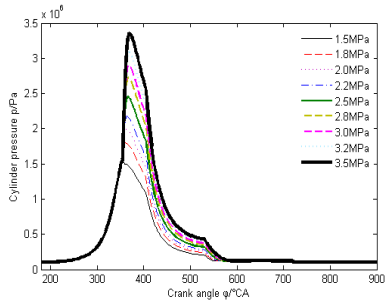

Fig.10 Cylinder pressure variation at different supply pressures

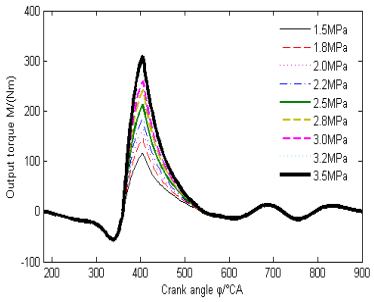

Fig.11 Output torque variation at different supply pressures

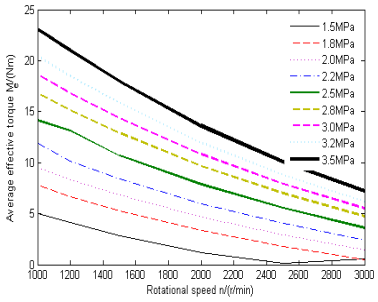

Fig.12 Average effective torque variation at different supply pressures

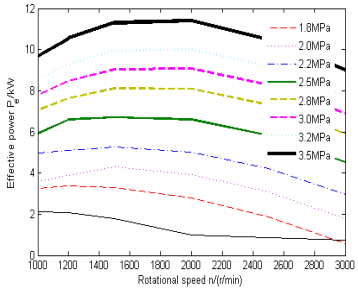

Fig.13 Effective power variation at different supply pressures

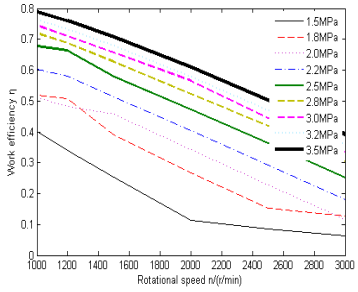

Fig.14 Work efficiency variation at different supply pressures

Supply pressure is another factor to affect working characteristics of the CAE. The cylinder pressure variation at different supply pressures is shown in Figure. 10. As observed from this figure, the increase of supply pressure results in a sharp increase of the top pressure of the cylinder, and the increase of the supply pressure results in pressure peak moving toward the larger crank angle. This is due to energy of compressed air increases as supply pressure increases without other influence factors, which means that the supply pressure has a positive effect on the dynamic performance of the CAE. The output torque variation at different supply pressures is shown in Figure. 11. Its variation tendency is the same as cylinder pressure. The larger the supply pressure, the larger the output torque. However, larger supply pressure leads to exhaust pressure is greater, which increases the reverse output torque of

the CAE. Under different supply pressure, the change rules of the relevant performance parameters are shown in Figure. 12~Figure. 14. With the same supply pressure condition, the increase of rotational speed is bad for increasing average effective torque and work efficiency, this indicates that the CAE is more suitable for lower rotational speed. Furthermore, it can be seen from Figure. 12 and Figure. 14 that average effective torque and work efficiency increase with the rising of supply pressure for the same rotational speed. Figure. 13 presents the working characteristics of the effective power at different supply pressures. From Figure. 13, one can find that effective power increases with the rising of supply pressure for the same rotational speed, and with the increased rotational speed, the change trend of effective power increases first and then decreases for the same supply pressure. On the whole, the rotational speed range of the effective power reaches the maximum is 1500r/min~2000r/min.

4.3 Supply temperature

The effect of supply temperature on working characteristics seems to be non-significant different with the range of whole work cycle. Figure. 15~Figure. 17 illustrated the variation of average effective torque, effective power and work efficiency under various supply temperatures. It is found that there is a slight variation of these characteristics parameters. As shown in these figures, with the increasing of supply temperature, their values will become smaller for the same rotational speed. Under the conditions of same supply temperature, average effective torque and work efficiency decrease with the increasing of rotational speed. The relationship between rotational speed and effective power is a parabola going downwards, when the effective power reaches the maximum, the rotational speed is about 1500r/min. According to the effect analysis of the supply temperature, increasing the supply temperature make little sense to power lift of the CAE, the key is to enhance heat transfer in the working process so as to improve the air temperature, thus improving the working performance of the CAE.

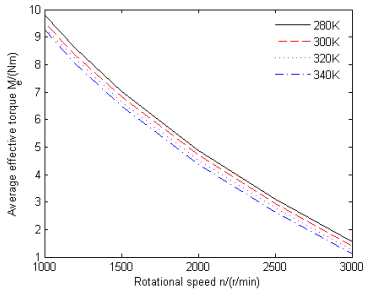

Fig. 15 Average effective torque variation at different supply temperatures

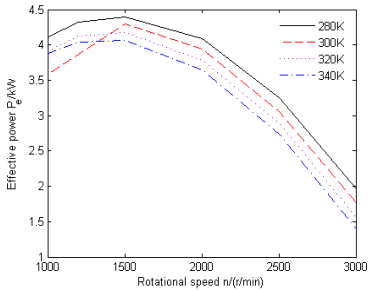

Fig.16 Effective power variation at different supply temperatures

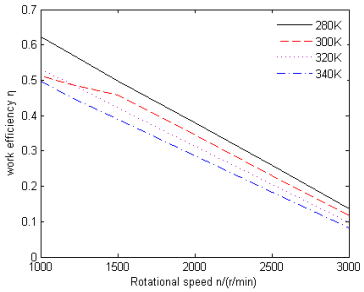

Fig. 17 Work efficiency variation at different supply temperatures

5. Conclusions

In this paper, a four-stroke compressed air engine is as a new research object is used to investigate the working performance. A mathematical model is developed to study the influence of several key performance parameters on working characteristics, and the experimental system is set up. The method of valid modeling is introduced to simulate real operating conditions, and the performance analysis on the influences of rotational speed, supply pressure and supply temperature are carried out. On the basis of the above analysis, some brief conclusions have been drawn.

(1) In the work process, the cylinder pressure and temperature rise rapidly during the compression stroke, then decrease gradually during the inflation and expansion stroke, and the air fluctuation is relatively stable during the exhaust stroke and intake stroke.

(2) The CAE has a higher cylinder pressure in the low speed stage and has the higher work efficiency, which is more suitable for low speed and stable condition.

(3) Compared with other working parameters, supply pressure has a greater influence on the performance of the CAE, and the increase of the supply pressure can effectively improve the indicated work and work efficiency.

(4) The supply temperature has little effect on the performance of the CAE, with the increasing of supply temperature, the average effective torque, effective power and work efficiency will decrease slightly.

It is obvious that the output torque, effective power and work efficiency of the CAE grow with the decrease of rotational speed and the increase of supply pressure. Not affecting the other performance, CAE may choose a higher supply pressure.

Acknowledgment

The authors would like to thank the automobile company SGMW in China for its kind assistance with the four-stroke IC engine fused for the present study. This research was supported by the Natural Science Foundation of China (Grant No. 11172220). The authors of the paper express their deep gratitude for the financial support of the research project.

References

[1] Li, Y. H., *et al*., Renewable Energy Carriers: Hydrogen or Liquid Air/Nitrogen?, *Applied Thermal Engineering, 30*,(2010), 14, pp. 1985–1990

[2] Foley, A., Lobera, I. D., Impacts of Comprssed Air Energy Storage Plant on an Electricity Market with A Large Renewable Energy Portfolio, *Energy, 57*,(2013), 8, pp. 85–94

[3] Zeng, F.C., Xu, J.L., Study on Exergy Analysis of A Compressed Air Engine, *Thermal Science, 22*,(2018), 3, pp. 1179–1191

[4] Liu, J. L., Wang, J. H., Thermodynamic Analysis of a Novel Tri-generation System Based on Compressed Air Energy Storage and Pneumatic Motor, *Energy, 91*,(2013), 11, pp. 420–429

[5] Shi, Y., *et al*., Literature Review: Present State and Future Trends of Air-Powered Vehicles, *Journal Renewable and Sustainable Energy, 8*,(2016), 2, pp. 325–342

[6] Yu, Q. H., *et al*., Dynamic Heat Transfer Model for Temperature Drop Analysis and Heat Exchange System Design of the Air-powered Engine System, *Energy, 68*,(2014), 4, pp. 877–885

[7] Huang, C. Y., *et al*., Experimental Investigation on the Performance of a Compressed-air Driven Piston Engine, *Energie, 6*,(13), 3, pp. 1713–1745

[8] Chen, Y., *et al*., Simulation on the Port Timing of an Air-powered Engine, *International Journal of Vehicle and Design, 38*,(2005), 2, pp. 259–273

[9] Liu, C.M., *et al*., Modified Intake and Exhaust System for Piston-type Compressed Air Engines,

Energy, *90*,(2015), pp. 516–524

[10] Liu, L., Yu, X.L., Practicality Study on Air-powered Vehicle, *Frontiers of Energy & Power Engineering in China*, *2*,(2008), 1, pp. 14–19

[11] Yu, Q.H., *et al*., Optimization of the Energy Efficiency of a Piston Compressed Air Engine, *Strojniški vestnik – J. Mechanical Engineering*, *60*,(2014), 6, pp. 395–406

[12] Yu, Q.H., *et al*., Working Characteristics of Two Types of Compressed Air Engine, *J. Renew. Sustain. Energy*, *8*,(2016), 3, pp. 397–411

[13] Yu, Q.H., *et al*., Dimensionless Study on Efficiency and Speed Characteristics of a Compressed Air Engine, *Journal of Energy resources technology-transactions of the ASME*, *137*,(2015), pp. 2181–2193

[14] Liu, C.M., *et al*., Performance Analysis of a Two-stage Expansion Air Engine, *Energy*, *115*,(2016), pp. 140–148

[15] Fang, Q.H. Numerical Simulation and Experimental Research on the Working Process of Hybrid Compressed-air and Fuel Engine. PhD thesis, Zhejiang University, China, 2009. (in Chinese)

[16] Xu, Z.G. Theoretical and Experimental Study of Adjustable Expansion Ratio Air Powered Engine. PhD thesis, South China University of Technology, China, 2014. (in Chinese)

[17] Xu, Q.Y., *et al*., Virtual Prototype Modeling and Performance Analysis of the Air-Powered Engine, *ARCHIVE Proceeding of the Institution of Mechanical Engineers*, 228,(2014), pp. 2642–2651

[18] Yu, Q.H., *et al*., Working Characteristics of Variable Intake Valve in Compressed Air Engine, *The Scientific World Journal*, 2014,(2014), pp. 1–9